



1 **IMPROVING THE SIMULATION OF GLOBAL AEROSOL WITH SIZE-**
2 **SEGREGATED ANTHROPOGENIC NUMBER EMISSIONS**

3 FILIPPO XAUSA¹, PAULI PAASONEN^{1,5}, RISTO MAKKONEN¹, MIKHAIL
4 ARSHINOV², AIJUN DING³, HUGO DENIER VAN DER GON⁴, VELI-MATTI
5 KERMINEN¹, MARKKU KULMALA¹

6 ¹ *Division of Atmospheric Sciences, Department of Physics, University of*
7 *Helsinki.*

8 ² *Institute of Atmospheric Optics, SB RAS, 634055, Tomsk, Russia.*

9 ³ *Joint International Research Laboratory of Atmospheric and Earth System*
10 *Sciences, School of Atmospheric Sciences, Nanjing University, Nanjing*
11 *210023, China.*

12 ⁴ *TNO, Department of Climate, Air and Sustainability, Utrecht, the*
13 *Netherlands.*

14 ⁵ *International Institute for Applied Systems Analysis (IIASA), Laxenburg,*
15 *Austria*

16

17

18 Keywords: AEROSOL, NUMBER SIZE DISTRIBUTION, GAINS, GLOBAL CLIMATE
19 MODEL

20

21

ABSTRACT

22 Climate models are important tools that are used for generating climate
23 change projections, in which aerosol-climate interactions are one of the main
24 sources of uncertainties. In order to quantify aerosol-radiation and aerosol-
25 cloud interactions, detailed input of anthropogenic aerosol number emissions
26 is necessary. However, the anthropogenic aerosol number emissions are
27 usually converted from the corresponding mass emissions in precompiled
28 emission inventories through a very simplistic method depending uniquely
29 on chemical composition, particle size and density, which are defined for a
30 few very wide main source sectors. In this work, the anthropogenic particle
31 number emissions converted from the AeroCom mass in the ECHAM-HAM



32 climate model were replaced with the recently-formulated number emissions
33 from the Greenhouse Gas and Air Pollution Interactions and Synergies
34 (GAINS)-model, where the emission number size distributions vary, for
35 example, with respect to the fuel and technology. A special attention in our
36 analysis was put on accumulation mode particles (particle diameter $d_p > 100$
37 nm) because of (i) their capability of acting as cloud condensation nuclei
38 (CCN), thus forming cloud droplets and affecting Earth's radiation budget,
39 and (ii) their dominant role in forming the coagulation sink and thus limiting
40 the concentration of sub-100 nanometers particles. In addition, the estimates
41 of anthropogenic CCN formation, and thus the forcing from aerosol-climate
42 interactions are expected to be affected. Analysis of global particle number
43 concentrations and size distributions reveal that GAINS implementation
44 increases CCN concentration compared with AeroCom, with regional
45 enhancement factors reaching values as high as 10. A comparison between
46 modeled and observed concentrations shows that the increase in number
47 concentration for accumulation mode particle agrees well with
48 measurements, but it leads to a consistent underestimation of both
49 nucleation mode and Aitken mode ($d_p < 100$ nm) particle number
50 concentrations. This suggests that revisions are needed in the new particle
51 formation and growth schemes currently applied in global modeling
52 frameworks.

53

54 1 Introduction

55 In recent years, the link between anthropogenic aerosol particle and climate
56 change has been a subject of several studies (e.g. Baker et al., 2015; Zhang
57 et al., 2016). Anthropogenic aerosol particles play an important role in the
58 global climate system via aerosol-radiation and aerosol-cloud interactions by
59 scattering and absorbing solar radiation and by acting as cloud condensation
60 or ice nuclei, thereby changing many cloud properties (Boucher et al., 2013).
61 The global and regional radiative effects of aerosol particles depend on the
62 spatial and temporal distribution of the aerosol number size distribution and
63 chemical composition (Lohmann and Feichter, 2005; Schulz et al., 2006;
64 Forster et al., 2007; Stier et al., 2007).

65 While anthropogenic primary emissions introduce cloud condensation nuclei
66 (CCN) directly into the atmosphere, a significant fraction of the global CCN
67 population is likely be formed through condensation of organic and other low-



68 volatility vapors onto ultra-fine particles (particle diameter $d_p < 100$ nm) in
69 the atmosphere (Spracklen et al., 2008; Merikanto et al., 2009; Kerminen et
70 al., 2012; Paasonen et al., 2013). Aerosol particles and their precursor vapors
71 are being emitted from both biogenic and anthropogenic sources, in addition
72 to which they may also result from interactions between biogenic and
73 anthropogenic emissions (Spracklen et al., 2011; Shilling et al., 2013). The
74 increasing number concentration of accumulation mode particles decreases
75 the formation and growth of smaller particles by increasing the sink for
76 condensing vapor molecules, termed the condensation sink (CS, Kulmala et
77 al., 2001), and by increasing the coagulation sink for small freshly-formed
78 particles. Hence, the number concentration of accumulation mode particles
79 from primary emissions affects secondary aerosol formation. The effects of
80 these physical processes on future aerosol climate forcing requires
81 application of detailed aerosol microphysical schemes in global climate
82 models. Furthermore, the global uncertainty in CCN is highly sensitive to the
83 assumed emission size distribution (Lee et al., 2013).

84 The global aerosol climate model ECHAM-HAM (Stier et al., 2005; Zhang et
85 al., 2012) is a useful tool that aims at increasing our understanding of
86 aerosol-climate interactions. Past simulations performed with the ECHAM-
87 HAM include an extensive analysis of particle nucleation (Makkonen et al.,
88 2009, 2014; Kazil et al., 2010), aerosol properties (Roelofs et al., 2010), and
89 emission data set implementation (Zhang et al., 2012). Although the ECHAM-
90 HAM has a detailed microphysics module for describing the aerosol size
91 distribution (Vignati et al., 2004), previous studies have not included an
92 exhaustive module for the input particle number size distribution. Also in
93 other climate models, the mass-only aerosol input is a commonly applied
94 setting (Jones et al., 2007; Shindell et al., 2007). The main reason behind this
95 resides in the structure of the input data rather than in the models
96 themselves.

97 One of the input emission inventories that has been widely used in ECHAM-
98 HAM simulations, as well as in other Earth System Models (Pozzoli et al.,
99 2011; Makkonen et al., 2009, 2012; Tonttila et al., 2015), is the Aerosol Inter
100 Comparison data set, AeroCom (Dentener et al., 2006), developed for the
101 purpose of conducting improved simulations of aerosol-climate interactions
102 (Samset et al., 2014). However, the AeroCom emission inventory does not
103 include a specific framework for particle number emissions. Hence, the input
104 particle number emissions used in the simulations with AeroCom are



105 estimated from the particle mass emissions by the ECHAM-HAM during the
106 initialization routine. In more detail, the estimation of number emissions
107 consists of a simplistic multiplication of the given AeroCom mass emissions
108 by a mass-to-number conversion factor. Each conversion factor that is
109 applied for building the log-normal distribution is calculated by assuming
110 that the mass emissions for each main source sector are distributed to
111 predefined modes according to predefined densities, geometric mean radii
112 and standard deviations, as described by Vignati et al., (2004) and Stier et
113 al., (2005). This simplistic mass-to-number conversion factor does not
114 represent the relationship between the particle mass and number size
115 distributions in a realistic way, because such framework does not take into
116 account the variation of emitted particle number size distributions from
117 different emitting sources. The AeroCom inventory includes anthropogenic
118 activities, from which the mass-to-number converted emissions are split into
119 half between the Aitken and accumulation modes, and finally converted into
120 log-normal modes. However, the recently-developed inventories allow for
121 global aerosol simulations with a more detailed aerosol emission size
122 distribution (Paasonen et al., 2016) with the GAINS emission scenario model
123 (Greenhouse gas - Air pollution INTERactions and Synergies; Cofala et al.,
124 2009; Amann et al., 2011). GAINS data are organized into more detailed
125 anthropogenic sources than AeroCom, with different particle number
126 emissions and size distributions related to different fuels and technologies.

127 In this work, we first develop a novel module for anthropogenic particle
128 number emissions in Earth System Models. Our experiment, performed with
129 ECHAM-HAM, consists of replacing the mass-to-number converted
130 anthropogenic AeroCom aerosol emissions with number emissions from the
131 GAINS-model. This study has a dual target: first, it aims at improving the
132 ECHAM-HAM capability for estimating particle number concentrations, with a
133 special focus on accumulation mode particles, and second, it investigates the
134 feasibility of using the GAINS model for global climate modeling studies by
135 running the ECHAM-HAM with both AeroCom and GAINS data sets. We will
136 make a comparison between AeroCom and GAINS in terms of emissions,
137 modeled particle number concentrations and size distributions, as well as
138 modeled CCN number concentrations. Finally, we will compare the modeled
139 number size distributions with observations in different environments around
140 the world.

141



142 2 Materials and methods

143 2.1 Model framework

144 2.1.1 The ECHAM5.5-HAM2 climate model

145 We used the global aerosol climate model ECHAM5.5-HAM2 (Stier et al.,
146 2005; Zhang et al., 2012) with M7 microphysics module (Vignati et al., 2004).
147 The M7 describes the aerosol number size distribution with seven log-normal
148 modes, in which the Aitken, accumulation and coarse modes are present in
149 both the soluble and insoluble phases, while the nucleation mode is present
150 only as the soluble mode. The compounds modeled in our simulations are
151 black carbon (BC), organic carbon (OC), sulfate (SO₄), dust and sea salt. The
152 emission module used in ECHAM-HAM reads data for anthropogenic,
153 biogenic, wildfire, volcanic, agricultural emissions, secondary organic
154 aerosols (SOA) and shipping sources. In our experiments, we modified only
155 the part of the ECHAM-HAM source code that handles the anthropogenic
156 emissions.

157 Our experiment consisted of two one-year simulations, using identical model
158 settings but different data set for anthropogenic sources: AeroCom and
159 GAINS (see Sect. 2.3). The experiment run was set to start indicatively on
160 October 1, 2009 and end on December 31, 2010 with a three-month spin-up
161 period and one-hour time resolution for the output. The modeled data for our
162 analysis were collected from January 1, 2010 to December 31, 2010. The
163 model was nudged against 2010 ECMWF ERA-Interim (Berrisford et al., 2011)
164 observed meteorology data in order to reduce noise in model estimations
165 and to increase the statistical significance of the eventual anthropogenic
166 aerosol perturbation signal (Kooperman et al., 2012). The model has a
167 horizontal gaussian grid (192×96) with a grid box size of ~200×200 km at
168 the equator, and a vertical resolution of 31 hybrid sigma layers.

169

170 2.1.2 Emission scenario model GAINS

171 The GAINS (Greenhouse gas - Air pollution Interactions and Synergies) model
172 is an integrated assessment model developed at IIASA (International Institute
173 for Applied Systems Analysis) in Laxenburg, Austria (Amann et al, 2011). In
174 order to calculate the emissions related to specific anthropogenic source
175 sectors, it combines the information of the annual level of the anthropogenic



176 activities, amounts of different fuels consumed for combustion activities,
177 shares of different emission abatement technologies, and emission factors
178 for different activity-fuel-technology-combinations.

179 The GAINS scenarios include information on the annual activity levels and
180 shares of emission control technologies for nearly 170 regions, being
181 countries or parts or groups of countries, in five-year intervals from 1990 to
182 2050. The activity levels are based on national and international statistics,
183 latter available from International Energy Agency (IEA), Organisation for
184 Economic Co-operation and Development (OECD), United Nations (UN) and
185 Food and Agriculture Organization of the United Nations (FAO) and Eurostat,
186 and the shares of control technologies are derived from national and
187 international information on the related legislation, discussion with national
188 experts and scientific publications. The emission factors for all combinations
189 of source sectors, fuels and technologies are determined from the scientific
190 publications or measurement databases. For detailed description of sources
191 and methods to derive underlying particulate matter emissions see Klimont
192 et al. (2016).

193 The particle number emission factors with the related number size
194 distributions were recently implemented to GAINS (Paasonen et al., 2016).
195 This implementation allowed for detailed assessment of particle number
196 emissions with more than 1000 measures controlling emissions in each of
197 the close to 170 regions, and in internally consistent manner with emissions
198 of other air pollutants and greenhouse gases. The GAINS particle number
199 emissions are known to be subject to uncertainties, especially in terms of
200 nucleation mode emissions, but the major particle number sources, such as
201 road transport and residential combustion, are reasonably well represented
202 down to the control technology level. The determination of emission factors
203 for particle number emissions and particle size distributions is based on the
204 European particle number emission inventory developed by TNO (Denier van
205 der Gon et al., 2009, 2010).

206 In this study, we applied the gridded emissions for year 2010 based on the
207 'ECLIPSE version 5' dataset (Klimont et al., 2016) developed within the EU
208 FP7 ECLIPSE project (Stohl et al., 2015). The gridded dataset and their brief
209 characterization is freely available from the IIASA website:

210 <http://www.iiasa.ac.at/web/home/research/researchPrograms/air/PN.html>.



211

212 2.2 Aerosol schemes

213 The version of ECHAM-HAM used in this work includes nucleation,
214 condensation and coagulation modules. Previous studies have shown that
215 the implementation of an activation-type nucleation improves particle
216 number concentration estimations in modeling (Spracklen et al., 2010;
217 Makkonen et al., 2012). In our experiment, we coupled a binary sulphuric
218 acid-water nucleation scheme (Vehkamäki et al., 2002) with an activation-
219 nucleation scheme described by Paasonen et al., (2010, Eq. 10), in which the
220 nucleation rate (J) is a function of the activation coefficient and sulphuric acid
221 concentration, expressed as

$$222 \quad J = 1.7 \times 10^{-6} \text{ s}^{-1} * [H_2SO_4] \quad (1)$$

223 The settings of our simulations included a specific module for SOA formation.
224 Here, we modeled the SOA formation with both kinetic condensation onto a
225 Fuchs-corrected surface area (CS) and partitioning according to a preexisting
226 organic mass (Riipinen et al., 2011; Jokinen et al., 2015). This SOA module
227 includes three biogenic volatile organic compound (BVOC) tracers: isoprene,
228 endocyclic monoterpenes and other monoterpenes, each having monthly
229 resolutions for emissions. We did not use any nucleation scheme for organic
230 vapors, because the simple activation-type nucleation, while not accurate for
231 individual sites, describes the nucleation in different environments
232 reasonably well (Paasonen et al., 2010). The particle growth from nucleation
233 size to the d_p of 3 nm was calculated according to Kerminen and Kulmala
234 (2002). BVOC emissions were implemented using the MEGAN2 (Guenther et
235 al., 2006) model. MEGAN2 estimates biogenic emissions for about 150
236 compounds from different ecosystems, paying a particular attention to
237 monoterpenes. This framework takes into account several factors that
238 influence BVOC emissions, including the leaf age, soil moisture and light
239 environment. MEGAN2 was run offline and its output data were used for the
240 ECHAM-HAM input initialization. More details can be found in Makkonen et al.
241 (2012).

242 Shipping emissions are embedded in the AeroCom data set, but not included
243 in GAINS. In our experiment, we masked out the AeroCom shipping emissions
244 with a land-sea mask produced by applying Climate Data Operator (CDO) to
245 the AeroCom. Hence, shipping emissions were not taken into consideration.



246 All non-anthropogenic emissions, such as volcanic emissions, dimethyl-
247 sulfide (DMS, Kloster et al., 2006) emitted by the sea and dust, were taken
248 from AeroCom in both simulations. All emission data, excluding SOA
249 precursors, DMS emissions and wildfire, were input as annual-averages. As a
250 result, the seasonality in concentrations of anthropogenic compounds is
251 mostly due to the nudged meteorology.

252

253 2.3 Anthropogenic Emissions

254 2.3.1 AeroCom

255 The first simulation was performed with the 2000 anthropogenic AeroCom
256 data set. The AeroCom emissions taken by the ECHAM-HAM are provided by
257 mass as $\text{kg m}^{-2} \text{s}^{-1}$ with a chemical differentiation that includes BC, OC and
258 SO_4 , and a bi-level vertical distribution (2-zL) that consists of two surface
259 layers: a lower level below 100 meters above the sea level for emissions
260 from transportation and domestic combustion, and a higher level for
261 industrial activities whose emissions reach altitudes higher than 100 meters.
262 While BC does not require preprocessing during the simulation, input
263 emissions of OC and SO_4 undergo a further conversion during the
264 initialization routine: OC mass is converted into primary organic matter
265 (POM) mass with a multiplying factor 1.4 (Turpin et al., 2000; Kupiainen and
266 Klimont, 2007), and emissions containing sulfur (S) are input as both sulfur
267 dioxide (SO_2) and SO_4 . The primary SO_4 -core particle fraction is estimated as
268 2.5% of gaseous SO_2 , as described by Dentener et al. (2006). The masses of
269 BC and POM are uniquely treated as Aitken mode particles ($d_p = 10\text{-}100 \text{ nm}$).
270 The mass of SO_4 is divided between the Aitken mode, accumulation mode (d_p
271 $= 100\text{-}1000 \text{ nm}$) and coarse mode ($d_p > 1 \mu\text{m}$) through a rough estimation:
272 the lower-surface-level SO_4 is split equally between the Aitken mode and
273 accumulation mode, whereas the higher-surface-level SO_4 is split equally
274 between the accumulation mode and coarse mode. The mass is then
275 converted by the model into a particle number size distribution. The mass-to-
276 number flux factors, expressed as $m2n$ in Figure 1, are embedded in the
277 emission-reading routine. The number of particles is calculated through the
278 generic function

$$279 \quad N = M/m \quad , \quad (2)$$



280 where M is the mass of given emissions and m is the average mass
281 estimated for a single particle. The particle mass m in Eq. (2) is extended in
282 the model according to the Hatch-Choate conversion equations (Hinds,
283 1982), in which the density, count median radius and standard deviation are
284 predefined for each chemical compound and size mode, as described by
285 Stier et al. (2005). The count median radius is fixed at 30 nm and 75 nm for
286 the Aitken mode and accumulation mode, respectively, and the standard
287 deviation is set to 1.59 for all the modes except the coarse mode for which it
288 is 2.0. The species density is set to 1841 kg m^{-3} for SO_4 (input in the model as
289 H_2SO_4) and 2000 kg m^{-3} for BC and OC. Altogether, these parameters
290 differentiate the species according to their chemistry and solubility. The
291 number flux conversion is therefore expressed as

$$292 \quad N = \frac{M}{\frac{4}{3} \cdot \pi \cdot \rho_i \cdot (\text{cmr}_{jk} \cdot \text{cmr}2\text{ram}_{jk})^3}, \quad (3)$$

293 where ρ is the density of a determined chemical compound i , and the
294 expression in brackets is the mean radius of a particle with certain solubility j
295 and size mode k . The quantity cmr is the predefined count median radius as
296 it is expressed in the model code, while $\text{cmr}2\text{ram}$ is a conversion factor that
297 multiplies cmr in order to estimate the radius of average mass. The $\text{cmr}2\text{ram}$
298 factor depends uniquely on the standard deviation of the log-normal particle
299 number distribution.

300

301 2.3.2 GAINS

302 In the second simulation, the sub-module that converts the input mass to the
303 number flux described in Eqs. (2-3) was switched off and we implemented
304 the recently-developed 2010 GAINS anthropogenic emissions (Paasonen et
305 al., 2016; see also section 2.1.2). The emission sectors considered for our
306 experiment included the energy production, flares, industrial combustion and
307 processes, transportation, waste combustion and domestic/commercial
308 combustion. A detailed description of the sectors and emission factors is
309 presented in Paasonen et al. (2016).

310 The number size distribution data provided by GAINS are organized into nine
311 size bins with a geometric diameter ranging from 3 nm to 1000 nm.
312 However, in this study we implemented the GAINS data for the Aitken mode



313 and accumulation mode only ($d_p = 10\text{-}1000$ nm), so that the particle number
314 implementation was consistent with the AeroCom simulation which lacked
315 the nucleation mode conversion factor in the source code aerosol module.
316 Therefore, in the GAINS simulation we kept the AeroCom data for the gas
317 phase sulfur and coarse SO_4 in order to identify the global impact of GAINS
318 implementation on submicron particles. Furthermore, we used the same bi-
319 level 2-zL scheme as for the SO_4 vertical distribution in AeroCom: emissions
320 from the transportation, agriculture fires, waste combustion and domestic
321 combustion were put into the lower level (<100 m a.s.l.), whereas the
322 energy, flares, industry and power plant sectors of GAINS were implemented
323 into the higher level (>100 m a.s.l.).

324 GAINS provides the number-only emission data without chemical speciation
325 and vertical distribution (see Table 1). Thus, we followed a series of steps in
326 order to partition the GAINS raw data into BC, POM and SO_4 in a consistent
327 format for the model. Table 1 and Figure 1 visually illustrate the
328 implementation framework. In more detail, we (I) off-line converted AeroCom
329 mass into number using ECHAM-HAM factors, (II) estimated the chemical
330 species fraction among the respective Aitken mode and accumulation mode
331 in AeroCom numbers, (III) applied such fractions to the total Aitken mode and
332 accumulation mode particle numbers in the GAINS to have the correspondent
333 BC, OC and SO_4 repartition, and finally, (IV) used the mass-to-number factors
334 used in (I) to estimate the speciated GAINS mass.

335

336 2.4 Comparison with observations

337 Our study focused on particle number concentration and size distributions
338 along with CCN concentrations at the supersaturations of 0.2% (CCN0.2) and
339 1.0% (CCN1.0). We compared the modeled particle number concentrations
340 and size distributions against observations collected from 11 sites around the
341 world. A detailed description of the observation data is illustrated in Table 2.
342 The modeled data extracted from all sites were averaged over the year and
343 plotted against observations to investigate the overall model performance.
344 The particle number concentration and mean particle radius of the whole
345 output data were used for plotting the number distributions from 6 of the 11
346 original sites, which were chosen to represent areas with a strong presence
347 of anthropogenic emissions (Nanjing, Sao Paulo and Tomsk) as well as areas
348 dominated by biogenic emissions (Hyytiälä, K-Pusztá and Värriö). In both



349 annual-average and number distribution comparisons, the modeled layer
350 closest to Earth's surface was chosen for analysis. Modeled CCN
351 concentrations were studied by comparing simulations with AeroCom
352 emissions against those from GAINS emissions for both CCN0.2 and CCN1.0.
353 CCN concentrations were extracted and averaged from the lowest three
354 model layers in order to reduce background noise in mapping the global
355 concentrations. Due to the coarse grid size and inhomogeneous sources
356 around measurement sites, the evaluation against observations is not
357 expected to yield one-to-one validation of aerosol concentrations (Schutgens
358 et al., 2016).

359

360 3 Results and discussion

361 Here we show the comparison between AeroCom and GAINS implementation
362 before (emissions, section 3.1) and after (atmospheric concentrations,
363 sections 3.2 and 3.3) running the ECHAM-HAM model. Our experiment was
364 performed with the same model settings in both simulations and it was
365 nudged against meteorology data. As a result, our analysis focused merely
366 on the differences between the particle number emissions of the two data
367 sets and their different effects on modeled particle concentrations. In the
368 following sections, we will first show the difference between AeroCom and
369 GAINS in terms of input emissions, after which we will compare the model-
370 simulated particle number concentrations and size distributions with
371 observational data. Finally, we will assess the effect of GAINS implementation
372 on global CCN concentrations.

373

374 3.1 Differences in particle number emissions

375 In this section, we present a preliminary assessment of input emissions to
376 illustrate the main differences between the two gridded data sets before
377 starting the simulation. Table 3 shows global emissions and their ratios
378 between GAINS and AeroCom for the whole domain. When the emissions
379 were globally averaged (R_{tot}), GAINS showed higher total number emissions
380 by a factor of 2.2. However, when looking at individual grid cells, the total
381 particle number emission ratios between Aerocom and GAINS had a large
382 spatial variability (Figure 2), even though the median value of this ratio was



383 very close to one (see R_{grid} in Table 3). Globally, the Aitken to accumulation
384 mode particle emission ratio was about two orders of magnitude in AeroCom
385 emissions, while being less than a factor four in GAINS emission. The
386 averaged emission ratios demonstrate that accumulation mode emissions
387 play a critical role in the GAINS implementation, with both R_{tot} and R_{grid}
388 ratios increasing dramatically compared with AeroCom. The averaged Aitken
389 mode particle emissions from GAINS did not show a similar increase, and the
390 R_{grid} median value was even lower than that in the AeroCom emissions. The
391 R_{tot} and R_{grid} ratios of Aitken mode emissions were 1.7 and 0.7, respectively.
392 This difference shows that the Aitken mode particle emissions are
393 quantitatively higher in GAINS than in AeroCom when their geographical
394 distribution differences are not taken into account. However, when the data
395 sets were compared by confronting each grid cell one by one, AeroCom
396 emissions were higher than GAINS in a prevalent area of the global domain.

397 It is important to mention that the high differences between GAINS and
398 AeroCom in terms of Aitken and accumulation mode emissions that are
399 presented in Table 3 are partly caused by the different shares of BC, OC, and
400 SO_4 in GAINS and AeroCom data sets. In the assumptions made for the
401 AeroCom emissions, fossil fuel and biofuel emissions are implemented in
402 Aitken mode only. In more detail, all BC emissions from AeroCom are
403 implemented in the M7 module as insoluble Aitken mode particles, which are
404 converted to soluble particles after sulfate condensation. The significant
405 difference in accumulation mode emissions and concentrations results from
406 non-existing accumulation emissions from fossil fuels and biofuels in the
407 AeroCom data set.

408

409 3.2 Simulated particle number concentrations and size distributions

410 Here we present the core of our analysis, which includes an assessment of
411 the modeled particle number concentrations against observations. Figure 4
412 shows the annual-averaged modeled particle concentration in comparison
413 with observations from eleven sites. Overall, both emission data sets showed
414 a tendency of underestimating particle number concentrations in model
415 simulations, especially for the locations having high observed particle
416 number concentrations. Underestimation of the highest particle
417 concentrations might be, at least partly, related to the spatial resolution of



418 ECHAM-HAM, due to which the typically high particle concentrations near
419 urban or industrial areas will be distributed evenly into a large model grid
420 cell (Stier et al., 2005). A comparison of the model results with the
421 observational data shows that the GAINS implementation significantly
422 improved the reproduction of observed concentrations in accumulation mode
423 ($d_p > 100$ nm), being closer to observations than AeroCom at all 11 sites. For
424 the Aitken mode ($d_p = 10$ -100 nm), similar improvement was not reached, as
425 the observed concentrations were better reproduced with AeroCom than with
426 GAINS at 8 sites.

427 Figure 5 shows the modeled particle number size distributions against
428 observations at 6 measurement sites. The size distributions modeled with
429 the GAINS emissions agreed relatively well with the measurements for the
430 accumulation mode, whereas the nucleation and Aitken modes were
431 underestimated in simulations with both emission data sets. GAINS
432 underestimated the Aitken mode particle concentrations more heavily than
433 AeroCom, by a factor of two to three in Hyytiälä, Värriö and Kpuszta,
434 suggesting that the higher condensation sink associated with higher
435 accumulation mode particle emissions in GAINS had a significant impact on
436 modeled ultra-fine particle number concentrations. In addition, Hyytiälä and
437 Värriö are regions in which BVOC emissions and clean air are the key
438 influencing factors for new particle formation and particle growth (Ruuskanen
439 et al., 2007; Corrigan et al., 2013; Liao et al., 2014). This was reflected in the
440 model results: particle number size distributions in Hyytiälä and Värriö were
441 quite similar between the two simulations based on different anthropogenic
442 emission data sets. Contrary to this, Nanjing, Sao Paulo and Tomsk are areas
443 with strong influences by anthropogenic emissions, so that in comparison
444 with AeroCom, the simulations with GAINS emissions produced higher
445 accumulation mode and Aitken mode particle number concentrations as well
446 as better agreements with the observations in these regions. Nevertheless,
447 the model was not able to reach the observed ultra-fine particle
448 concentration in either simulation in most areas, and the higher CS in GAINS
449 significantly reduced particle number concentrations of the smallest particles
450 in most regions. Some areas showed a dramatic reduction in simulated ultra-
451 fine particle number concentrations e.g. in Nanjing the whole modeled
452 nucleation mode was wiped out when using the GAINS emissions.

453 The above results suggest that in ECHAM-HAM, as well as probably in other
454 climate models, the current nucleation and growth schemes may need



455 further revisions. However, it is also likely that the anthropogenic emissions
456 of especially nucleation mode particles in GAINS are still severely
457 underestimated for many source sectors (Paasonen et al., 2016). This is
458 because many of the measurements, on which the GAINS emission factors
459 are based, are not sensitive to non-solid nucleation mode particles, such as
460 those formed via nucleation of sulfur or organic vapors immediately after the
461 combustion or at small downwind distances in plumes from different
462 combustion sources (Stevens and Pierce, 2013). In addition, the lower
463 modeled Aitken mode particle concentrations from GAINS emissions may, in
464 some parts of the global domain, be also related to possible overestimations
465 in the accumulation mode particle emissions in the GAINS model, which are
466 consequently affecting the formation and growth of smaller particles.
467 Nonetheless, all the model versus observation comparisons between the
468 simulations clearly represent a consistent challenge for climate models in
469 modeling ultra-fine particle number size distributions.

470 Figure 6 shows absolute annual-average particle concentrations for the
471 accumulation mode and Aitken mode with both AeroCom and GAINS
472 emissions. While the regional distributions had similar patterns in both
473 simulations, there were evident differences when looking at the two size
474 modes. Accumulation mode particle concentrations were higher for the
475 simulation with the GAINS emission in most regions, which is consistent with
476 the input emissions assessment. The differences were particularly evident
477 over the developing areas where anthropogenic activities represent the main
478 source of atmospheric particle, especially in South America, central Africa,
479 India, China and south-east Asia. As observed in Figure 5, the high
480 accumulation mode particle number concentrations in the simulation with
481 the GAINS emission has a critical effect on Aitken mode particle
482 concentrations at most sites. A peculiar pattern is observed in China where
483 the dominant presence of anthropogenic sources from GAINS led the model
484 to predict high concentrations of ultra-fine particles. The decrease in GAINS-
485 derived Aitken mode particle number concentrations in areas where
486 emissions were actually higher than the AeroCom emission implies that
487 Aitken mode particles had been removed, or their secondary production was
488 hindered, by the prominent increase of the CS caused by a higher number of
489 emitted accumulation mode particles.

490



491 3.3 Concentrations and sources of CCN

492 This section presents the impact of particle emission data on atmospheric
493 CCN concentrations on annual and seasonal perspectives. It is important to
494 note that the applied anthropogenic number emissions did not have a
495 seasonal variation, so the seasonal differences are entirely due to the
496 variation of other emissions, and mainly to the strong temperature
497 dependence of biogenic SOA formation affecting the CCN concentration
498 (Paasonen et al., 2013). Our results showed clear differences in the simulated
499 CCN concentrations between the two primary emission data sets, and these
500 differences depended strongly on the considered supersaturation (Figure 7
501 and 8).

502 At the 0.2% supersaturation, the CCN concentrations were higher with the
503 GAINS emissions compared with the AeroCom emissions in practically all the
504 regions and during all seasons (Figure 8). The annual-average CCN_{0.2}
505 concentration ratio between the GAINS and AeroCom was two to three in
506 most areas, with peaks of four to ten in south America, central Africa and
507 east Asia (Figure 7). However, a significant fraction of the global
508 accumulation mode particle concentration was observed in India, China and
509 south-east Asia (see Figure 6), and thus the increase in absolute CCN_{0.2}
510 concentration due to anthropogenic emissions is largest in eastern China and
511 south-east Asia. Our analysis of the seasonality revealed that the difference
512 between GAINS and AeroCom simulations in terms of CCN_{0.2} concentrations
513 was the largest during the cold season in January, with boreal and arctic
514 regions showing an increment of GAINS/AeroCom CCN_{0.2} ratio up to a factor
515 of seven to ten. The southern hemisphere also displayed notable differences
516 in both South America and South-East Asia, with GAINS/AeroCom CCN_{0.2}
517 ratios of three to ten during the warmest season.

518 At the supersaturation of 1.0%, a significant fraction of Aitken mode particles
519 is capable of acting as CCN. Opposite to the CCN_{0.2} concentrations, the
520 simulated CCN_{1.0} concentrations with the GAINS emissions were lower than
521 with AeroCom emissions, with a GAINS/AeroCom ratio between 0.5 and 1 in
522 most regions (Figure 7). Our seasonality analysis showed that the simulation
523 with the GAINS data set produced higher CCN_{1.0} concentrations than
524 AeroCom in Europe, India and East Asia during the winter. However, such
525 ratio was equal to one or below in most regions, except eastern Asia, during
526 the warmer seasons. The substantially lower CCN_{1.0} concentrations with



527 GAINS emissions arise from the relatively similar Aitken mode number
528 emissions between GAINS and AeroCom, but significantly larger CS from
529 GAINS causing a decrease in secondary ultrafine particle formation.
530 However, in China and South-East Asia, the annual CCN1.0 concentration
531 from GAINS was higher than from AeroCom by at least a factor of two,
532 suggesting that these regions may play a key role in contributing for the
533 global anthropogenic emissions and increment of CCN.

534 It is important to remark that the substantial differences in CCN
535 concentrations illustrated above are linked to the implementation of different
536 data sets, and therefore the modeled estimations might be affected by
537 uncertainties of the GAINS model as well. Furthermore, it may be questioned
538 whether the ECHAM-HAM is actually able to estimate CCN concentrations
539 with GAINS better than with AeroCom. This goes beyond the fundamental
540 goal of this study, which is to address the feasibility of using GAINS
541 emissions in global climate modeling. However, the modeled GAINS
542 accumulation mode particle number concentrations agree with observation
543 significantly better than AeroCom. This, based on the sensitivity analysis by
544 Lee et al. (2013), suggests that the GAINS implementation is likely to
545 estimate CCN concentrations better than AeroCom. In any case, further
546 studies are needed to address the tangible contribution of the GAINS model
547 in improving modeled CCN concentration. Furthermore, it would be beneficial
548 to investigate how the applied nucleation scheme, combined with the GAINS
549 anthropogenic emissions, affects the estimation of CCN concentration to
550 better identify the driving forces behind the uncertainties of modeling
551 particle number size distributions with the global climate models.

552

553 Conclusions

554 The outcome of our experiment shows that the most significant differences
555 between the GAINS and AeroCom emissions data sets are (i) the particle size
556 distribution in the Aitken mode and accumulation mode, and (ii) the
557 geographical distribution of the particle number emissions over the global
558 domain. The accumulation mode particle emissions from GAINS are
559 significantly higher than AeroCom, by factors from 10 to 1000, thus
560 potentially resulting in dramatic increases of climatically active primary
561 particles and simultaneous decreases in secondary ultrafine particle
562 formation due to higher values of CS and coagulation sink.



563 In comparison to AeroCom emissions, GAINS emissions produced much
564 higher accumulation mode particle concentrations, but the consequently
565 higher CS and coagulation sink led to lower Aitken mode concentrations with
566 GAINS emissions than with AeroCom emissions. In comparison to observation
567 data at eleven measurement sites, the modeled annual-averaged
568 concentrations with GAINS emissions performed better than with AeroCom
569 emissions, in terms of bringing the modeled accumulation mode particle
570 concentrations closer to observation at all eleven sites, and Aitken mode
571 particle concentrations closer to observation at three sites. However, higher
572 underestimation was observed in the simulation with GAINS emissions for
573 particles with $d_p < 30$ nm.

574 The underestimation of $d_p < 30$ nm particle concentrations in the simulation
575 with GAINS emissions highlighted the sensitivity of nucleation mode and
576 Aitken mode particle concentrations to CS and coagulation sink. This
577 underestimation is presumably partly caused by underestimations in
578 emissions of non-solid nucleation/Aitken mode particles in the GAINS model
579 (Paasonen et al., 2016). As a first next step, the nucleation parameterizations
580 and the sensitivity of the concentrations of sulfuric acid (the main precursor
581 in the applied nucleation parameterization) to altered CS should be revised.

582 It is important to note that the simulations performed in this study did not
583 implement an up-to-date secondary organic aerosols (ELVOCS) nucleation
584 scheme, which may represent a further step to reduce the gap between the
585 modeled and observed concentrations. Finally, given the high spatial
586 variability of global emissions, more observation data and the establishment
587 of new measurement stations in varying environments are urgently needed
588 to better evaluate the model results.

589

590 Acknowledgements

591 This project was funded by the MAJ JA TOR NESSLING grant n. 201600369
592 and the Academy of Finland Center of Excellence (FCoE) grant n. 307331.

593 Particle number size distributions at Melpitz were provided by Wolfram
594 Birmili, Kay Weinhold, André Sonntag, Birgit Wehner, Thomas Tuch, and
595 Alfred Wiedensohler (Leibniz Institute for Tropospheric Research, Leipzig,
596 Germany).



597 Particle number size distributions at Hohenpeissenberg were provided by
598 Harald Flentje and Björn Briel (German Weather Service, Hohenpeissenberg,
599 Germany). Both measurements were supported by the German Federal
600 Environment Ministry (BMU) grant UFOPLAN 370343200, project duration
601 2008-2010. Both data sets can be publicly accessed through the German
602 Ultrafine Aerosol Network (GUAN) at <https://doi.org/10.5072/guan>.

603 Particle number size distributions at Botsalano were provided by Ville Vakkari
604 and Lauri Laakso (Finnish Meteorological Institute, Helsinki, Finland).

605 Particle number size distributions at Sao Paulo were provided by John
606 Backman (Finnish Meteorological Institute, Helsinki, Finland).

607 Particle number size distributions at San Pietro Capofiume (Po Valley) were
608 provided by Ari Laaksonen (Finnish Meteorological Institute, Helsinki,
609 Finland).

610 We thank Chris Heyes and Zbigniew Klimont from the Air Quality and
611 Greenhouse Gases program at IIASA, and Kaarle Kupiainen from IIASA and
612 Finnish Environment Institute (SYKE) for their help and communication.

613 The EU FP7 BACCHUS project (grant n. 603445) and the Nordic Center of Excellence
614 eSTICC (Nordforsk grant n. 57001 are acknowledged for financial support.

615

616

617

618

619

620

621

622

623

624

625



626

REFERENCES

- 627 Amann, M., Bertok, I., Borcken-Kleefeld, J., Cofala, J., Heyes, C., Höglund-Isaksson, L., Klimont,
628 Z., Nguyen, B., Posch, M., Rafaj, P., Sandler, R., Schöpp, W., Wagner, F. and Winiwarter, W.:
629 Cost-effective control of air quality and greenhouse gases in Europe: Modeling and policy
630 applications, *Environ. Model. Softw.*, 26(2), 1489-1501, 2011.
631
632 Backman, J., Rizzo, L. V., Hakala, J., Nieminen, T., Manninen, H. E., Morais, F., Aalto, P. P.,
633 Siivola, E., Carbone, S., Hillamo, R., Artaxo, P., Virkkula, A., Petäjä, T., and Kulmala, M.: On the
634 diurnal cycle of urban aerosols, black carbon and the occurrence of new particle formation
635 events in springtime São Paulo, Brazil, *Atmos. Chem. Phys.*, 12, 11733-11751,
636 doi:10.5194/acp-12-11733-2012, 2012.
637
638 Baker, L. H., Collins, W. J., Olivie, D. J. L., Cherian, R., Hodnebrog, Ø., Myhre, G., and Quaas,
639 J.: Climate responses to anthropogenic emissions of short-lived climate pollutants, *Atmos.*
640 *Chem. Phys.*, 15, 8201-8216, doi:10.5194/acp-15-8201-2015, 2015.
641
642 Berrisford, P., Kållberg, P., Kobayashi, S., Dee, D., Uppala, S., Simmons, A. J., Poli, P. and Sato,
643 H.: Atmospheric conservation properties in ERA-Interim. *Quarterly Journal of the Royal*
644 *Meteorological Society* 137:1381-1399, 2011.
645
646 Birmili, W., Weinhold, K., Rasch, F., Sonntag, A., Sun, J., Merkel, M., Wiedensohler, A., Bastian,
647 S., Schladitz, A., Löschau, G., Cyrys, J., Pitz, M., Gu, J., Kusch, T., Flentje, H., Quass, U.,
648 Kaminski, H., Kuhlbusch, T. A. J., Meinhardt, F., Schwerin, A., Bath, O., Ries, L., Gerwig, H.,
649 Wirtz, K., and Fiebig, M.: Long-term observations of tropospheric particle number size
650 distributions and equivalent black carbon mass concentrations in the German Ultrafine
651 Aerosol Network (GUAN), *Earth Syst. Sci. Data*, 8, 355-382, doi:10.5194/essd-8-355-2016,
652 2016.
653
654 Boucher, O., Randall, D., Artaxo, P., Bretherton, C., Feingold, G., Forster, P., Kerminen, V.-M.,
655 Kondo, Y., Liao, H., Lohmann, U., Rasch, P., Satheesh, S.K., Sherwood, S., Stevens, B. and
656 Zhang, X.Y.: Clouds and aerosols. In *Climate Change 2013: The Physical Science Basis.*
657 *Contribution of Working Group I to the Fifth Assessment Report of the Intergovernmental*
658 *Panel on Climate Change.* T.F. Stocker, D. Qin, G.-K. Plattner, M. Tignor, S.K. Allen, J.
659 Doschung, A. Nauels, Y. Xia, V. Bex, and P.M. Midgley, Eds. Cambridge University Press, 571-
660 657, doi:10.1017/CBO9781107415324.016, 2013.
661
662 Corrigan, A. L., Russell, L. M., Takahama, S., Äijälä, M., Ehn, M., Junninen, H., Rinne, J., Petäjä,
663 T., Kulmala, M., Vogel, A. L., Hoffmann, T., Ebben, C. J., Geiger, F. M., Chhabra, P., Seinfeld, J.
664 H., Worsnop, D. R., Song, W., Auld, J., and Williams, J.: Biogenic and biomass burning organic
665 aerosol in a boreal forest at Hyytiälä, Finland, during HUMPPA-COPEC 2010, *Atmos. Chem.*
666 *Phys.*, 13, 12233-12256, doi:10.5194/acp-13-12233-2013, 2013.
667
668 Dal Maso M., Sogacheva L., Anisimov M. P., Arshinov M., Baklanov A., Belan B., Khodzher T.
669 V., Obolkin V. A., Staroverova A., Vlasov A., Zagaynov V. A., Lushnikov A., Lyubovtseva Y. S.,
670 Riipinen I., Kerminen V.-M. and Kulmala M.: Aerosol particle formation events at two Siberian
671 stations inside the boreal forest. *Boreal Env. Res.* 13, 81-92, 2008.
672
673 Denier van der Gon, H., Visschedijk, A., Johansson, C., Hedberg Larsson, E., Harrison, R. M.,
674 and Beddows, D.: Size-resolved Pan European Anthropogenic Particle Number Inventory,
675 EUCAARI Deliverable 141, 2009.
676



- 677 Denier van der Gon, H., Visschedijk, A., Johansson, C., Ntziachristos, L., and Harrison, R. M.:
678 Size-resolved Pan-European Anthropogenic Particle Number Inventory, paper presented at
679 International Aerosol conference (oral), 29 August 3 September 2010, Helsinki, 2010.
680
- 681 Dentener, F., Kinne, S., Bond, T., Boucher, O., Cofala, J., Generoso, S., Ginoux, P., Gong, S.,
682 Hoelzemann, J. J., Ito, A., Marelli, L., Penner, J. E., Putaud, J.-P., Textor, C., Schulz, M., van der
683 Werf, G. R., and Wilson, J.: Emissions of primary aerosol and precursor gases in the years
684 2000 and 1750 prescribed data-sets for AeroCom, Atmos. Chem. Phys., 6, 4321-4344,
685 doi:10.5194/acp-6-4321-2006, 2006.
686
- 687 Forster, P., Ramaswamy, V., Artaxo, P., Berntsen, T., Betts, R., Fahey, D.W., Haywood, J., Lean,
688 J., Lowe, D.C., Myhre, G., Nganga, J., Prinn, R., Raga, G., Schulz, M., Van Dorland, R. and
689 Miller, H.L.: *Changes in Atmospheric Constituents and in Radiative Forcing Chapter 2*. United
690 Kingdom: Cambridge University Press, 2007.
691
- 692 Guenther, A., Karl, T., Harley, P., Wiedinmyer, C., Palmer, P. I., and Geron, C.: Estimates of
693 global terrestrial isoprene emissions using MEGAN (Model of Emissions of Gases and
694 Aerosols from Nature), Atmos. Chem. Phys., 6, 3181-3210, doi:10.5194/acp-6- 3181-2006,
695 2006.
696
- 697 Gultepe, I. Isaac, G.A.: Scale Effects on Averaging of Cloud Droplet and Aerosol Number
698 Concentrations: Observations and Models. J. Climate 12:1268-1279, 1999.
699
- 700 Hamed, A., Joutsensaari, J., Mikkonen, S., Sogacheva, L., Dal Maso, M., Kulmala, M., Cavalli,
701 F., Fuzzi, S., Facchini, M. C., Decesari, S., Mircea, M., Lehtinen, K. E. J., and Laaksonen, A.:
702 Nucleation and growth of new particles in Po Valley, Italy, Atmos. Chem. Phys., 7, 355-376,
703 doi:10.5194/acp-7-355-2007, 2007.
- 704 Hari P., Kulmala M., Pohja T., Lahti T., Siivola E., Palva L., Aalto P., Hämeri K., Vesala T.,
705 Luoma S. and Pulliainen E.: Air pollution in Eastern Lapland: challenge for an
706 environmental measurement station. Silva Fennica 28: 29-39, 1994.
- 707 Hari, P. & Kulmala, M. Station for Measuring Ecosystem-Atmosphere Relations (SMEAR II).
708 Boreal Env. Res., 10, 315-322, 2005.
- 709 Herrmann, E., Ding, A. J., Kerminen, V.-M., Petäjä, T., Yang, X. Q., Sun, J. N., Qi, X. M.,
710 Manninen, H., Hakala, J., Nieminen, T., Aalto, P. P., Kulmala, M., and Fu, C. B.: Aerosols and
711 nucleation in eastern China: first insights from the new SORPES-NJU station, Atmos. Chem.
712 Phys., 14, 2169-2183, doi:10.5194/acp-14-2169-2014, 2014.
713
- 714 Hinds, W. C. (1982) Aerosol Technology, p. 85. Wiley, New York.
715
- 716 IPCC, Climate Change: The Physical Science Basis. Contribution of Working Group I to the
717 Fifth Assessment Report of the Intergovernmental Panel on Climate Change [Stocker, T.F., D.
718 Qin, G.-K. Plattner, M. Tignor, S.K. Allen, J. Boschung, A. Nauels, Y. Xia, V. Bex and P.M.
719 Midgley (eds.)]. Cambridge University Press, Cambridge, United Kingdom and New York, NY,
720 USA, 1535 pp, doi:10.1017/CBO9781107415324, 2013.
721
- 722 Jones, A., Haywood, J. M. and Boucher, O.: Aerosol forcing, climate response and climate
723 sensitivity in the Hadley Centre climate model, J. Geophys. Res., 112, D20211,
724 doi:10.1029/2007JD008688, 2007.
725



- 726 Jokinen, T., Berndt, T., Makkonen, R., Kerminen, V., Junninen, H., Paasonen, P., Stratmann, F.,
727 Herrmann, H., Guenther, A.B., Worsnop, D.R., Kulmala, M., Ehn, M., Sipilä, M.: Production of
728 extremely low volatile organic compounds from biogenic emissions: Measured yields and
729 atmospheric implications, *Proceedings of the National Academy of Sciences* 112:7123-7128,
730 2015.
- 731
- 732 Kazil, J., Stier, P., Zhang, K., Quaas, J., Kinne, S., O'Donnell, D., Rast, S., Esch, M., Ferrachat,
733 S., Lohmann, U., and Feichter, J.: Aerosol nucleation and its role for clouds and Earth's
734 radiative forcing in the aerosol-climate model ECHAM5-HAM, *Atmos. Chem. Phys.*, 10,
735 10733-10752, doi:10.5194/acp-10-10733-2010, 2010.
- 736
- 737 Kerminen, V.-M., Kulmala, M.: Analytical formulae connecting the "real" and the "apparent"
738 nucleation rate and the nuclei number concentration for atmospheric nucleation events. *J*
739 *Aerosol Sci* 33(4):609-622, 2002.
- 740
- 741 Kerminen, V.-M., Paramonov, M., Anttila, T., Riipinen, I., Fountoukis, C., Korhonen, H., Asmi,
742 E., Laakso, L., Lihavainen, H., Swietlicki, E., Svenningsson, B., Asmi, A., Pandis, S. N.,
743 Kulmala, M., and Petäjä, T.: Cloud condensation nuclei production associated with
744 atmospheric nucleation: a synthesis based on existing literature and new results, *Atmos.*
745 *Chem. Phys.*, 12, 12037-12059, doi:10.5194/acp-12-12037-2012, 2012.
- 746
- 747 Kinne, S., Schulz, M., Textor, C., Guibert, S., Balkanski, Y., Bauer, S. E., Bernsten, T., Berglen,
748 T. F., Boucher, O., Chin, M., Collins, W., Dentener, F., Diehl, T., Easter, R., Feichter, J., Fillmore,
749 D., Ghan, S., Ginoux, P., Gong, S., Grini, A., Hendricks, J., Herzog, M., Horowitz, L., Isaksen, I.,
750 Iversen, T., Kirkevåg, A., Kloster, S., Koch, D., Kristjansson, J. E., Krol, M., Lauer, A.,
751 Lamarque, J. F., Lesins, G., Liu, X., Lohmann, U., Montanaro, V., Myhre, G., Penner, J., Pitari,
752 G., Reddy, S., Seland, O., Stier, P., Takemura, T., and Tie, X.: An AeroCom initial assessment -
753 optical properties in aerosol component modules of global models, *Atmos. Chem. Phys.*, 6,
754 1815-1834, doi:10.5194/acp-6-1815-2006, 2006.
- 755
- 756 Kiss, G., Varga, B., Galambos, I., & Ganszky, I. Characterization of water-soluble organic
757 matter isolated from atmospheric fine aerosol. *J. Geophys. Res.*, 107, 8339-8347,
758 doi:10.1029/2001JD000603, 2002.
- 759
- 760 Klimont, Z., Kupiainen, K., Heyes, C., Purohit, P., Cofala, J., Rafaj, P., Borken-Kleefeld, J. and
761 Schöpp, W.: Global anthropogenic emissions of particulate matter including black carbon,
762 *Atmospheric Chem. Phys. Discuss.*, 2016, 1-72, doi:10.5194/acp-2016-880, 2016.
- 763
- 764 Kloster, S., Feichter, J., Maier-Reimer, E., Six, K. D., Stier, P., and Wetzal, P.: DMS cycle in the
765 marine ocean-atmosphere system - a global model study, *Biogeosciences*, 3, 29-51,
766 doi:10.5194/bg-3-29-2006, 2006.
- 767
- 768 Kooperman, G. J., Pritchard, M. S., Ghan, S. J., Wang, M., Somerville, R. C. J., and Russell, L.
769 M.: Constraining the influence of natural variability to improve estimates of global aerosol
770 indirect effects in a nudged version of the Community Atmosphere Model 5, *J. Geophys. Res.*,
771 117, D23204, doi:10.1029/2012JD018588, 2012.
- 772
- 773 Kulmala, M., Dal Maso, M., Mäkelä, J., Pirjola, L., Väkevä, M., Aalto, P., Miikkulainen, P.,
774 Hämeri, K., and O'dowd, C.: On the formation, growth and composition of nucleation mode
775 particles. *Tellus B*, 53(4). doi:<http://dx.doi.org/10.3402/tellusb.v53i4.16622>, 2001.

776



- 777 Kupiainen, K. and Klimont, Z.: Primary emissions of fine carbonaceous particles in Europe.
778 Atmospheric Environment 41:2156 – 2170, 2007.
779
- 780 Laakso, L., Laakso, H., Aalto, P. P., Keronen, P., Petäjä, T., Nieminen, T., Pohja, T., Siivola, E.,
781 Kulmala, M., Kgabi, N., Molefe, M., Mabaso, D., Phalatse, D., Pienaar, K., and Kerminen, V.-M.:
782 Basic characteristics of atmospheric particles, trace gases and meteorology in a relatively
783 clean Southern African Savannah environment, Atmos. Chem. Phys., 8, 4823-4839,
784 doi:10.5194/acp-8-4823-2008, 2008.
785
- 786 Lee, L. A., Pringle, K. J., Reddington, C. L., Mann, G. W., Stier, P., Spracklen, D. V., Pierce, J. R.,
787 and Carslaw, K. S.: The magnitude and causes of uncertainty in global model simulations of
788 cloud condensation nuclei, Atmos. Chem. Phys., 13, 8879-8914, doi:10.5194/acp-13-8879-
789 2013, 2013.
790
- 791 Liao, L., Kerminen, V.-M., Boy, M., Kulmala, M., and Dal Maso, M.: Temperature influence on
792 the natural aerosol budget over boreal forests, Atmos. Chem. Phys., 14, 8295-8308,
793 doi:10.5194/acp-14-8295-2014, 2014.
794
- 795 Lohmann, U. and Feichter, J.: Global indirect aerosol effects: a review, Atmos. Chem. Phys.,
796 5, 715-737, doi:10.5194/acp-5-715-2005, 2005.
797
- 798 Makkonen, R., Asmi, A., Korhonen, H., Kokkola, H., Järvenoja, S., Räisänen, P., Lehtinen, K. E.
799 J., Laaksonen, A., Kerminen, V.-M., Järvinen, H., Lohmann, U., Bennartz, R., Feichter, J., and
800 Kulmala, M.: Sensitivity of aerosol concentrations and cloud properties to nucleation and
801 secondary organic distribution in ECHAM5-HAM global circulation model, Atmos. Chem.
802 Phys., 9, 1747-1766, doi:10.5194/acp-9-1747-2009, 2009.
803
- 804 Makkonen, R., Asmi, A., Kerminen, V.-M., Boy, M., Arneth, A., Guenther, A., and Kulmala, M.:
805 BVOC-aerosol-climate interactions in the global aerosol-climate model ECHAM5.5-HAM2,
806 Atmos. Chem. Phys., 12, 10077-10096, doi:10.5194/acp-12-10077-2012, 2012.
807
- 808 Makkonen, R., Seland, Ø., Kirkevåg, A., Iversen, T., and Kristjánsson, J. E.: Evaluation of
809 aerosol number concentrations in NorESM with improved nucleation parameterization,
810 Atmos. Chem. Phys., 14, 5127-5152, doi:10.5194/acp-14-5127-2014, 2014.
811
- 812 Merikanto, J., Spracklen, D. V., Mann, G. W., Pickering, S. J., and Carslaw, K. S.: Impact of
813 nucleation on global CCN, Atmos. Chem. Phys., 9, 8601-8616, doi:10.5194/acp-9-8601-2009,
814 2009.
815
- 816 Paasonen, P., Asmi, A., Petaja, T., Kajos, M.K, Aijala, M, Junninen, H, Holst, T, Abbatt, J.P.D,
817 Arneth, A, Birmili, W, van der Gon, H.D, Hamed, A, Hoffer, A, Laakso, L, Laaksonen, A,
818 Richard Leaitch, W, Plass-Dulmer, C, Pryor, S.C, Raisanen, P, Swietlicki, E, Wiedensohler, A,
819 Worsnop, D.R, Kerminen, V, Kulmala, M.: Warming-induced increase in aerosol number
820 concentration likely to moderate climate change. Nature Geoscience 6:438-442, 2013.
821
- 822 Paasonen, P., Kupiainen, K., Klimont, Z., Visschedijk, A., Denier van der Gon, H. A. C., and
823 Amann, M.: Continental anthropogenic primary particle number emissions, Atmos. Chem.
824 Phys., 16, 6823-6840, doi:10.5194/acp-16-6823-2016, 2016.
825
- 826 Pozzoli, L., Janssens-Maenhout, G., Diehl, T., Bey, I., Schultz, M. G., Feichter, J., Vignati, E.,
827 and Dentener, F.: Re-analysis of tropospheric sulfate aerosol and ozone for the period 1980–
828 2005 using the aerosol-chemistry-climate model ECHAM5-HAMMOZ, Atmos. Chem. Phys., 11,
829 9563-9594, doi:10.5194/acp-11-9563-2011, 2011.



- 830
831 Riipinen, I., Pierce, J. R., Yli-Juuti, T., Nieminen, T., Häkkinen, S., Ehn, M., Junninen, H.,
832 Lehtipalo, K., Petäjä, T., Slowik, J., Chang, R., Shantz, N. C., Abbatt, J., Leaitch, W. R.,
833 Kerminen, V.-M., Worsnop, D. R., Pandis, S. N., Donahue, N. M., and Kulmala, M.: Organic
834 condensation: a vital link connecting aerosol formation to cloud condensation nuclei (CCN)
835 concentrations, *Atmos. Chem. Phys.*, 11, 3865-3878, doi:10.5194/acp-11-3865-2011, 2011.
836
837 Roelofs, G.-J., ten Brink, H., Kiendler-Scharr, A., de Leeuw, G., Mensah, A., Minikin, A., and
838 Otjes, R.: Evaluation of simulated aerosol properties with the aerosol-climate model
839 ECHAM5-HAM using observations from the IMPACT field campaign, *Atmos. Chem. Phys.*, 10,
840 7709-7722, doi:10.5194/acp-10-7709-2010, 2010.
841
842 Ruuskanen, T. M., Kaasik, M., Aalto, P. P., Hörrak, U., Vana, M., Mårtensson, M., Yoon, Y. J.,
843 Keronen, P., Mordas, G., Ceburnis, D., Nilsson, E. D., O'Dowd, C., Noppel, M., Alliksaar, T.,
844 Ivask, J., Sofiev, M., Prank, M., and Kulmala, M.: Concentrations and fluxes of aerosol
845 particles during the LAPBIAT measurement campaign at Värriö field station, *Atmos. Chem.*
846 *Phys.*, 7, 3683-3700, doi:10.5194/acp-7-3683-2007, 2007.
847
848 Samset, B. H., Myhre, G., Herber, A., Kondo, Y., Li, S.-M., Moteki, N., Koike, M., Oshima, N.,
849 Schwarz, J. P., Balkanski, Y., Bauer, S. E., Bellouin, N., Berntsen, T. K., Bian, H., Chin, M., Diehl,
850 T., Easter, R. C., Ghan, S. J., Iversen, T., Kirkevåg, A., Lamarque, J.-F., Lin, G., Liu, X., Penner, J.
851 E., Schulz, M., Seland, Ø., Skeie, R. B., Stier, P., Takemura, T., Tsigaridis, K., and Zhang, K.:
852 Modelled black carbon radiative forcing and atmospheric lifetime in AeroCom Phase II
853 constrained by aircraft observations, *Atmos. Chem. Phys.*, 14, 12465-12477,
854 doi:10.5194/acp-14-12465-2014, 2014.
855
856 Schulz, M., Textor, C., Kinne, S., Balkanski, Y., Bauer, S., Berntsen, T., Berglen, T., Boucher, O.,
857 Dentener, F., Guibert, S., Isaksen, I. S. A., Iversen, T., Koch, D., Kirkevåg, A., Liu, X.,
858 Montanaro, V., Myhre, G., Penner, J. E., Pitari, G., Reddy, S., Seland, Ø., Stier, P., and
859 Takemura, T.: Radiative forcing by aerosols as derived from the AeroCom present-day and
860 pre-industrial simulations, *Atmos. Chem. Phys.*, 6, 5225-5246, doi:10.5194/acp-6-5225-2006,
861 2006.
862
863 Schurgers, G., Arneth, A., Holzinger, R., and Goldstein, A. H.: Process-based modelling of
864 biogenic monoterpene emissions combining production and release from storage, *Atmos.*
865 *Chem. Phys.*, 9, 3409-3423, doi:10.5194/acp-9-3409-2009, 2009.
866
867 Schutgens, N. A. J., Gryspeerdt, E., Weigum, N., Tsyro, S., Goto, D., Schulz, M., and Stier, P.:
868 Will a perfect model agree with perfect observations? The impact of spatial sampling, *Atmos.*
869 *Chem. Phys.*, 16, 6335-6353, doi:10.5194/acp-16-6335-2016, 2016.
870
871 Seinfeld, J. H. and Pandis, S. N.: *Atmospheric Chemistry and Physics: From Air Pollution to*
872 *Climate Change*, John Wiley and Sons, 1998.
873
874 Shilling, J. E., Zaveri, R. A., Fast, J. D., Kleinman, L., Alexander, M. L., Canagaratna, M. R.,
875 Fortner, E., Hubbe, J. M., Jayne, J. T., Sedlacek, A., Setyan, A., Springston, S., Worsnop, D. R.,
876 and Zhang, Q.: Enhanced SOA formation from mixed anthropogenic and biogenic emissions
877 during the CARES campaign, *Atmos. Chem. Phys.*, 13, 2091-2113, doi:10.5194/acp-13-2091-
878 2013, 2013.
879
880 Shindell, D. T., Faluvegi, G., Bauer, S. E., Koch, D. M., Unger, N., Menon, S., Miller, R. L.,
881 Schmidt, G. A. and Streets, D. G.: Climate response to projected changes in short-lived



- 882 species under an A1B scenario from 2000–2050 in the GISS climate model, *J. Geophys. Res.*,
883 112, D20103, doi:10.1029/2007JD008753, 2007.
- 884
- 885 Spracklen, D. V., Carslaw, K. S., Kulmala, M., Kerminen, V.-M., Mann, G. W., and Sihto, S.-L.:
886 The contribution of boundary layer nucleation events to total particle concentrations on
887 regional and global scales, *Atmos. Chem. Phys.*, 6, 5631–5648, doi:10.5194/acp-6-5631-
888 2006, 2006.
- 889
- 890 Spracklen, D. V., Carslaw, K. S., Kerminen, V.-M., Sihto, S.-L., Riipinen, I., Merikanto, J., Mann,
891 G. W., Chipperfield, M. P., Wiedensohler, A., Birmili, W. and Lihavainen, H.: Contribution of
892 particle formation to global cloud condensation nuclei concentrations, *Geophys. Res.*
893 *Letts.*, 35, L06808, doi:10.1029/2007GL033038.
- 894
- 895 Spracklen, D. V., Carslaw, K. S., Merikanto, J., Mann, G. W., Reddington, C. L., Pickering, S.,
896 Ogren, J. A., Andrews, E., Baltensperger, U., Weingartner, E., Boy, M., Kulmala, M., Laakso, L.,
897 Lihavainen, H., Kivekäs, N., Komppula, M., Mihalopoulos, N., Kouvarakis, G., Jennings, S. G.,
898 O'Dowd, C., Birmili, W., Wiedensohler, A., Weller, R., Gras, J., Laj, P., Sellegri, K., Bonn, B.,
899 Krejci, R., Laaksonen, A., Hamed, A., Minikin, A., Harrison, R. M., Talbot, R., and Sun, J.:
900 Explaining global surface aerosol number concentrations in terms of primary emissions and
901 particle formation, *Atmos. Chem. Phys.*, 10, 4775–4793, doi:10.5194/acp-10-4775-2010,
902 2010.
- 903
- 904 Spracklen, D. V., Jimenez, J. L., Carslaw, K. S., Worsnop, D. R., Evans, M. J., Mann, G. W.,
905 Zhang, Q., Canagaratna, M. R., Allan, J., Coe, H., McFiggans, G., Rap, A., and Forster, P.:
906 Aerosol mass spectrometer constraint on the global secondary organic aerosol budget,
907 *Atmos. Chem. Phys.*, 11, 12109–12136, doi:10.5194/acp-11-12109-2011, 2011.
- 908
- 909 Stevens, R. G. and Pierce, J. R.: A parameterization of sub-grid particle formation in sulfur-
910 rich plumes for global- and regional-scale models, *Atmos. Chem. Phys.*, 13, 12117–12133,
911 doi:10.5194/acp-13-12117-2013, 2013.
- 912
- 913 Stier, P., Feichter, J., Kinne, S., Kloster, S., Vignati, E., Wilson, J., Ganzeveld, L., Tegen, I.,
914 Werner, M., Balkanski, Y., Schulz, M., Boucher, O., Minikin, A., and Petzold, A.: The aerosol-
915 climate model ECHAM5-HAM, *Atmos. Chem. Phys.*, 5, 1125–1156, doi:10.5194/acp-5-1125-
916 2005, 2005.
- 917
- 918 Stier, P., Seinfeld, J. H., Kinne, S., and Boucher, O.: Aerosol absorption and radiative forcing,
919 *Atmos. Chem. Phys.*, 7, 5237–5261, doi:10.5194/acp-7-5237-2007, 2007.
- 920
- 921 Stohl, A., Aamaas, B., Amann, M., Baker, L. H., Bellouin, N., Berntsen, T. K., Boucher, O.,
922 Cherian, R., Collins, W., Daskalakis, N., Dusinska, M., Eckhardt, S., Fuglestad, J. S., Harju,
923 M., Heyes, C., Hodnebrog, Ø., Hao, J., Im, U., Kanakidou, M., Klimont, Z., Kupiainen, K., Law,
924 K. S., Lund, M. T., Maas, R., MacIntosh, C. R., Myhre, G., Myriokefalitakis, S., Olivie, D., Quaas,
925 J., Quennehen, B., Raut, J.-C., Rumbold, S. T., Samset, B. H., Schulz, M., Seland, Ø., Shine, K.
926 P., Skeie, R. B., Wang, S., Yttri, K. E., and Zhu, T.: Evaluating the climate and air quality
927 impacts of short-lived pollutants, *Atmos. Chem. Phys.*, 15, 10529–10566, doi:10.5194/acp-
928 15-10529-2015, 2015.
- 929
- 930 Textor, C., Schulz, M., Guibert, S., Kinne, S., Balkanski, Y., Bauer, S., Berntsen, T., Berglen, T.,
931 Boucher, O., Chin, M., Dentener, F., Diehl, T., Easter, R., Feichter, H., Fillmore, D., Ghan, S.,
932 Ginoux, P., Gong, S., Grini, A., Hendricks, J., Horowitz, L., Huang, P., Isaksen, I., Iversen, I.,
933 Kloster, S., Koch, D., Kirkevåg, A., Kristjansson, J. E., Krol, M., Lauer, A., Lamarque, J. F., Liu,
934 X., Montanaro, V., Myhre, G., Penner, J., Pitari, G., Reddy, S., Seland, Ø., Stier, P., Takemura,



- 935 T., and Tie, X.: Analysis and quantification of the diversities of aerosol life cycles within
936 AeroCom, Atmos. Chem. Phys., 6, 1777-1813, doi:10.5194/acp-6-1777-2006, 2006.
937
- 938 Tonttila, J., Järvinen, H., and Räisänen, P.: Explicit representation of subgrid variability in
939 cloud microphysics yields weaker aerosol indirect effect in the ECHAM5-HAM2 climate model,
940 Atmos. Chem. Phys., 15, 703-714, doi:10.5194/acp-15-703-2015, 2015.
941
- 942 Tsigaridis, K., Daskalakis, N., Kanakidou, M., Adams, P. J., Artaxo, P., Bahadur, R., Balkanski,
943 Y., Bauer, S. E., Bellouin, N., Benedetti, A., Bergman, T., Berntsen, T. K., Beukes, J. P., Bian, H.,
944 Carslaw, K. S., Chin, M., Curci, G., Diehl, T., Easter, R. C., Ghan, S. J., Gong, S. L., Hodzic, A.,
945 Hoyle, C. R., Iversen, T., Jathar, S., Jimenez, J. L., Kaiser, J. W., Kirkevåg, A., Koch, D., Kokkola,
946 H., Lee, Y. H., Lin, G., Liu, X., Luo, G., Ma, X., Mann, G. W., Mihalopoulos, N., Morcrette, J.-J.,
947 Müller, J.-F., Myhre, G., Myriokefalitakis, S., Ng, N. L., O'Donnell, D., Penner, J. E., Pozzoli, L.,
948 Pringle, K. J., Russell, L. M., Schulz, M., Sciare, J., Seland, Ø., Shindell, D. T., Sillman, S., Skeie,
949 R. B., Spracklen, D., Stavrakou, T., Steenrod, S. D., Takemura, T., Tiitta, P., Tilmes, S., Tost, H.,
950 van Noije, T., van Zyl, P. G., von Salzen, K., Yu, F., Wang, Z., Wang, Z., Zaveri, R. A., Zhang,
951 H., Zhang, K., Zhang, Q., and Zhang, X.: The AeroCom evaluation and intercomparison of
952 organic aerosol in global models, Atmos. Chem. Phys., 14, 10845-10895, doi:10.5194/acp-
953 14-10845-2014, 2014.
954
- 955 Turpin, B.J., Saxena, P., Andrews, E.: Measuring and simulating particulate organics in the
956 atmosphere: problems and prospects. Atmospheric Environment 34:2983-3013, 2000.
957
- 958 van Ulden, A. and Wieringa, J.: Atmospheric boundary layer re- search at Cabauw, Bound.-
959 Lay. Meteorol., 78, 39-69, 1996.
960
- 961 Vignati, E., Wilson, J. and Stier, P.: M7: An efficient size-resolved aerosol microphysics module
962 for large-scale aerosol transport models, J. Geophys. Res., 109, D22202,
963 doi:10.1029/2003JD004485, 2004.
964
- 965 Zhang, K., O'Donnell, D., Kazil, J., Stier, P., Kinne, S., Lohmann, U., Ferrachat, S., Croft, B.,
966 Quaas, J., Wan, H., Rast, S., and Feichter, J.: The global aerosol-climate model ECHAM-HAM,
967 version 2: sensitivity to improvements in process representations, Atmos. Chem. Phys., 12,
968 8911-8949, doi:10.5194/acp-12-8911-2012, 2012.
969
- 970 Zhang, S., Wang, M., Ghan, S. J., Ding, A., Wang, H., Zhang, K., Neubauer, D., Lohmann, U.,
971 Ferrachat, S., Takeamura, T., Gettelman, A., Morrison, H., Lee, Y., Shindell, D. T., Partridge, D.
972 G., Stier, P., Kipling, Z., and Fu, C.: On the characteristics of aerosol indirect effect based on
973 dynamic regimes in global climate models, Atmos. Chem. Phys., 16, 2765-2783,
974 doi:10.5194/acp-16-2765-2016, 2016.
975
976
977
978
979
980
981
982
983
984
985



986

TABLES

987

988 Table 1. Input data provided from AeroCom inventory and GAINS model for submicron
989 particle emissions. The data is sorted according to its original structure in terms of mass,
990 number, chemical species differentiation (BC, OC and SO₄), bi-level vertical distribution (2-
991 zL) and base year. (✓) and (x) indicate whether the data set contains a certain information
992 or not, respectively.

Data	M	N	Species	2-zL	Year
AeroCom	✓	x	✓	✓	2000
GAINS	x	✓	x	x	2010

993

994

995

996

997

998

999

1000

1001

1002

1003

1004

1005

1006

1007

1008

1009

1010



1011 Table 2. Description of measurement sites for model versus observation evaluation.

Station	Lon	Lat	m. a. s. l.	Years	Reference
Botsalano, South Africa	25.8 ° E	25.5 ° S	1424	07/2006-08/2007	Laakso et al., 2008.
Cabauw, Netherlands	4.9 ° E	52.0 ° N	60	04/2008-03/2009	van Ulden and Wieringa, 1996.
Hohenpeissenberg, Germany	11.0 ° E	47.8 ° N	980	06/2007-11/2008	Birmili et al., 2016.
Hyytiälä, Finland	24.3 ° E	61.9 ° N	180	01/2009-12/2010	Hari and Kulmala, 2005.
K-Puszta, Hungary	19.6 ° E	47.0 ° N	125	03/2007-03/2009	Kiss et al., 2002.
Melpitz, Germany	12.9 ° E	51.5 ° N	84	01/2007-12/2008	Birmili et al., 2016.
Nanjing, China	118.9 ° E	32.1 ° N	40	12/2011-12/2014	Herrmann et al., 2014.
Po Valley, Italy	11.6 ° E	44.7 ° N	11	09/2004-09/2006	Hamed et al., 2007.
Sao Paulo, Brazil	46.7 ° W	23.5 ° S	760	10/2010-09/2011	Backman et al., 2012.
Tomsk, Russia	84.1 ° E	56.4 ° N	80	01/2012-12/2013	Dal Maso et al., 2008.
Värriö, Finland	29.6 ° E	67.8 ° N	400	01/2009-12/2011	Hari et al., 1994.

1012



1013 Table 3. Total particle number (second and third columns) and global average ratios (fourth
 1014 and fifth columns) of input emissions computed for the whole domain. R_{tot} ratios are
 1015 calculated by firstly averaging the emissions among the whole domain for each data set,
 1016 and secondly divide GAINS by AeroCom. This method aims at studying absolute differences
 1017 in the global emissions with no regard to geographical distribution differences. In R_{grid} we
 1018 firstly divide the data sets to keep the information of data sets differences for each grid cell,
 1019 and secondly compute the median of gridded ratios.

Global emissions	AeroCom $10^9 \text{ m}^{-2} \text{ s}^{-1}$	GAINS $10^9 \text{ m}^{-2} \text{ s}^{-1}$	R_{tot} mean	R_{grid} median
Total	7.23	15.63	2.16	1.00
Accumulation	0.06	3.68	59.18	48.65
Aitken	7.17	11.96	1.67	0.71

1020

1021

1022 Table 4. Modeled global annually-averaged concentrations of total particle, CCN0.2 and
 1023 CCN1.0 with AeroCom and GAINS data sets (second and third columns). Continental and
 1024 (global) average ratios of total particle and CCN concentrations were calculated as in Table
 1025 3.

Global concentrations	AeroCom 10^{12} m^{-3}	GAINS 10^{12} m^{-3}	R_{tot} mean	R_{grid} median
Total	37.08	33.98	0.83 (0.91)	0.96 (0.99)
CCN0.2	1.65	2.47	1.69 (1.49)	1.16 (1.04)
CCN1.0	7.04	6.77	0.96 (0.96)	0.99 (0.98)

1026

1027

1028

1029

1030

1031

1032

1033

1034

1035

1036

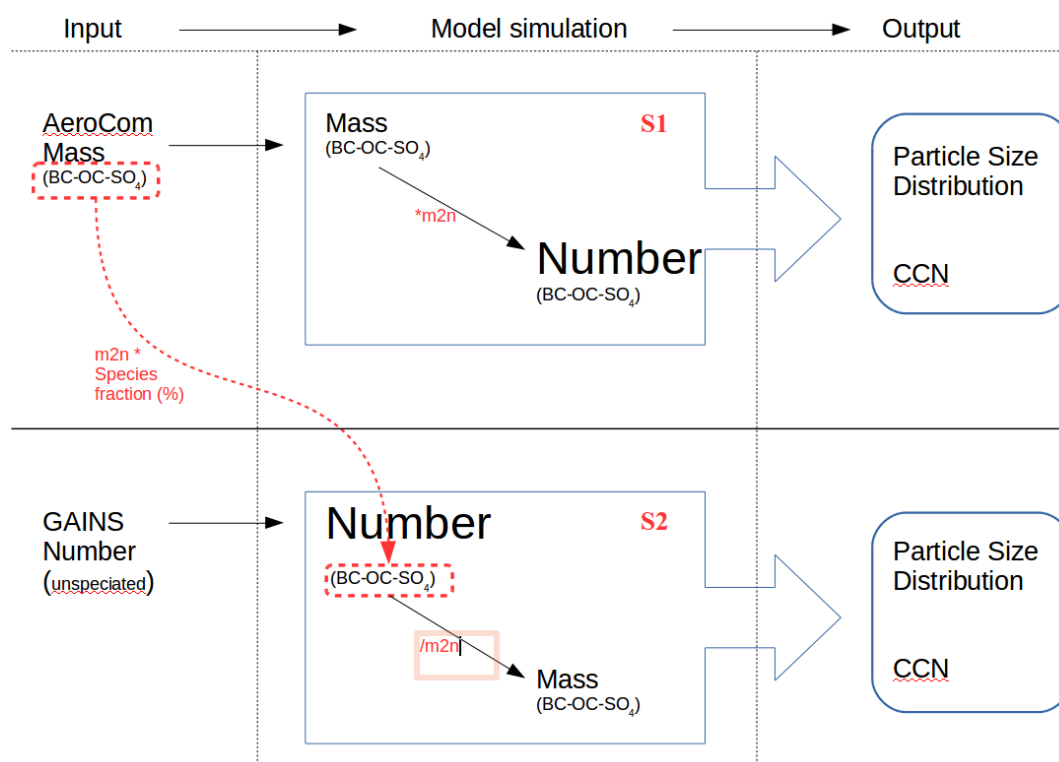
1037

1038



1039
 1040

FIGURES



1042 Figure 1. Framework describing the off-line steps to implement GAINS mass and number
 1043 anthropogenic emissions in the ECHAM-HAM. The AeroCom mass-to-number (m2n)
 1044 conversion factors and the chemical species fractions (%) of AeroCom number emissions
 1045 were used to speciate GAINS number emissions. A specific m2n factor was used for each
 1046 species for either mass-to-number (*m2n) or number-to-mass (/m2n) conversion.

1047
 1048

1049

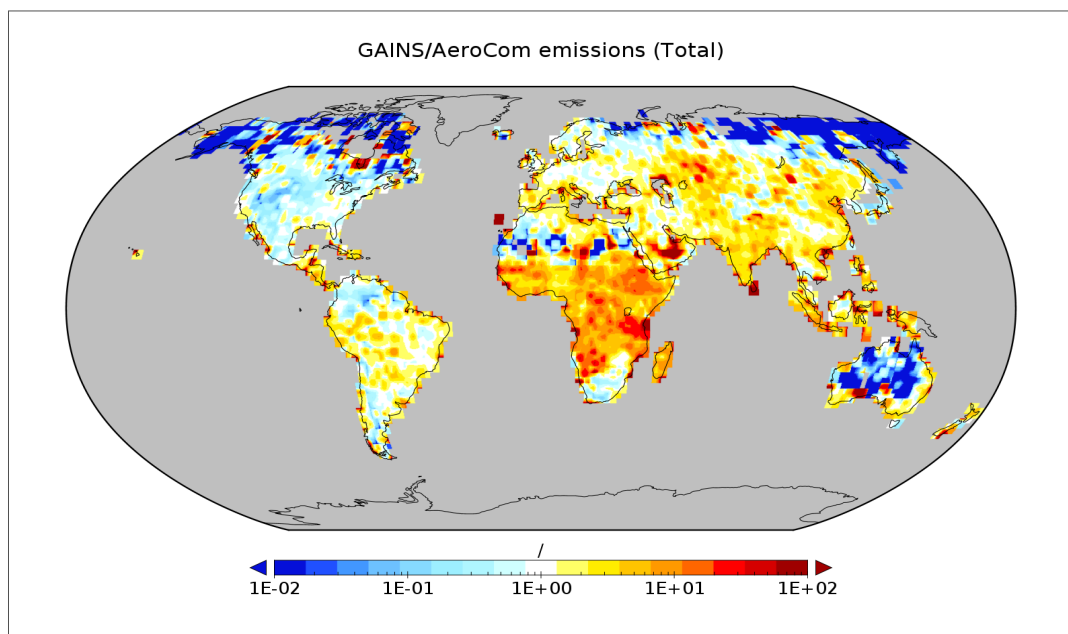
1050

1051

1052

1053

1054



1055 Figure 2. GAINS/AeroCom ratio for annual particle number emissions.

1056

1057

1058

1059

1060

1061

1062

1063

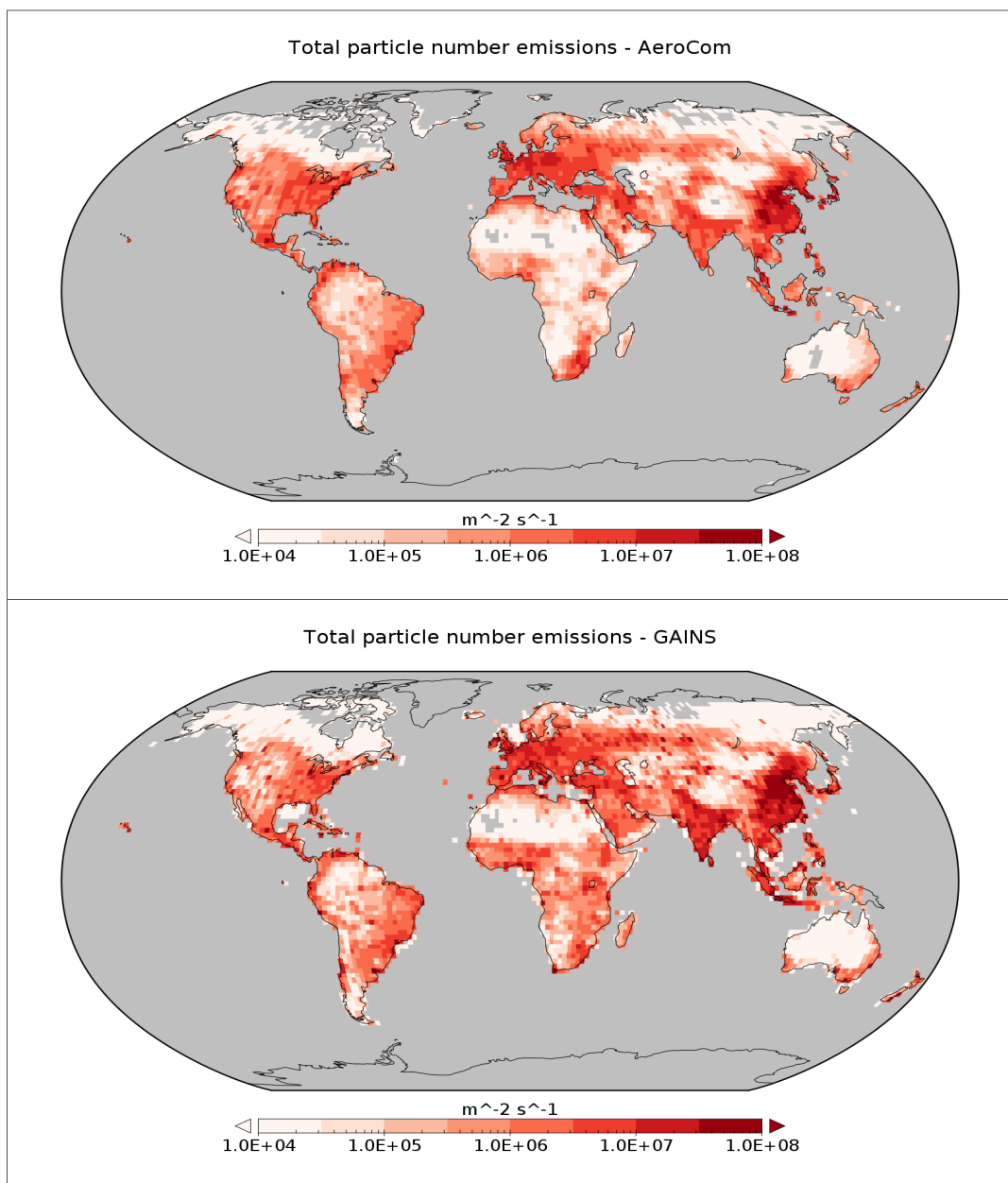
1064

1065

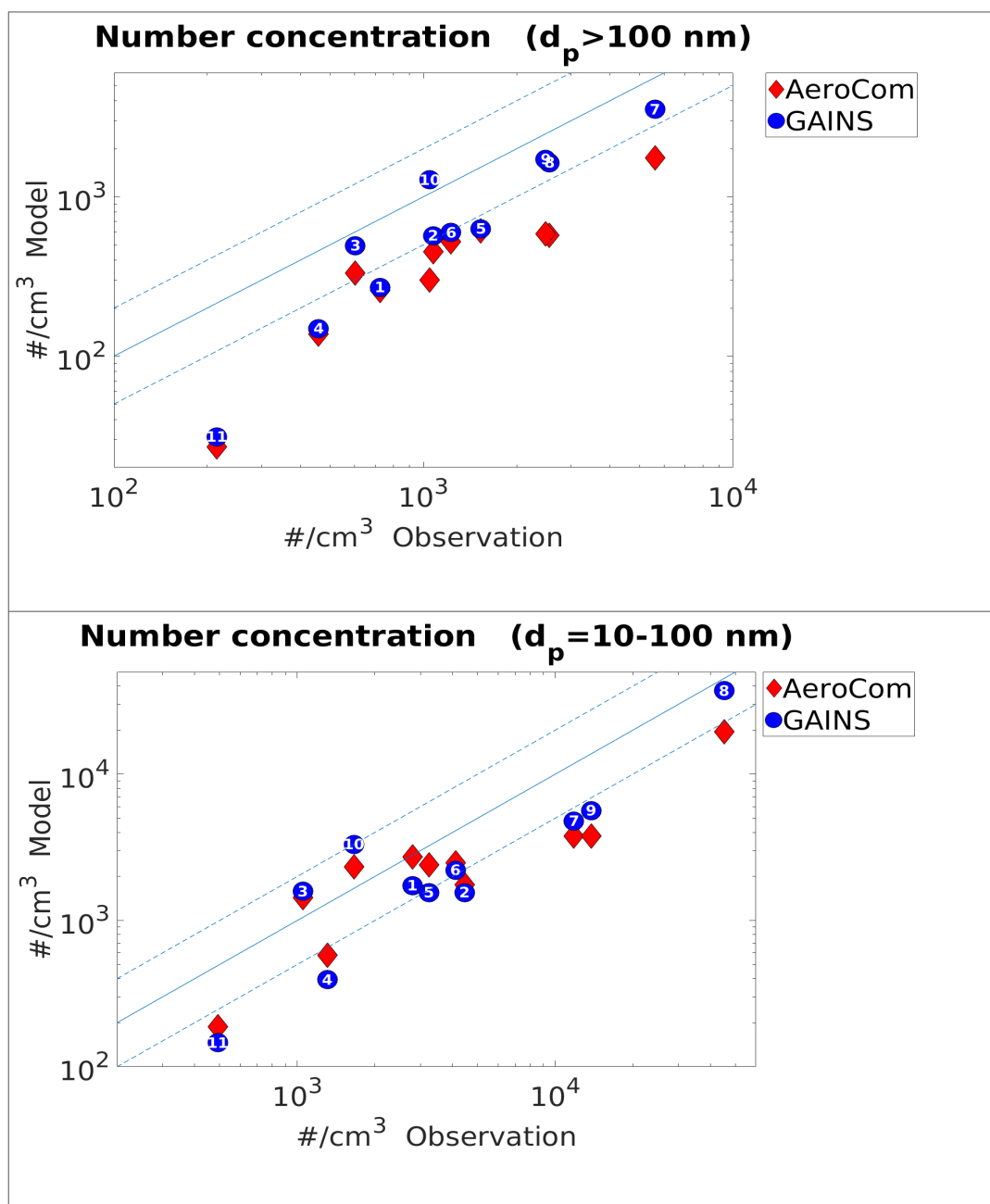
1066

1067

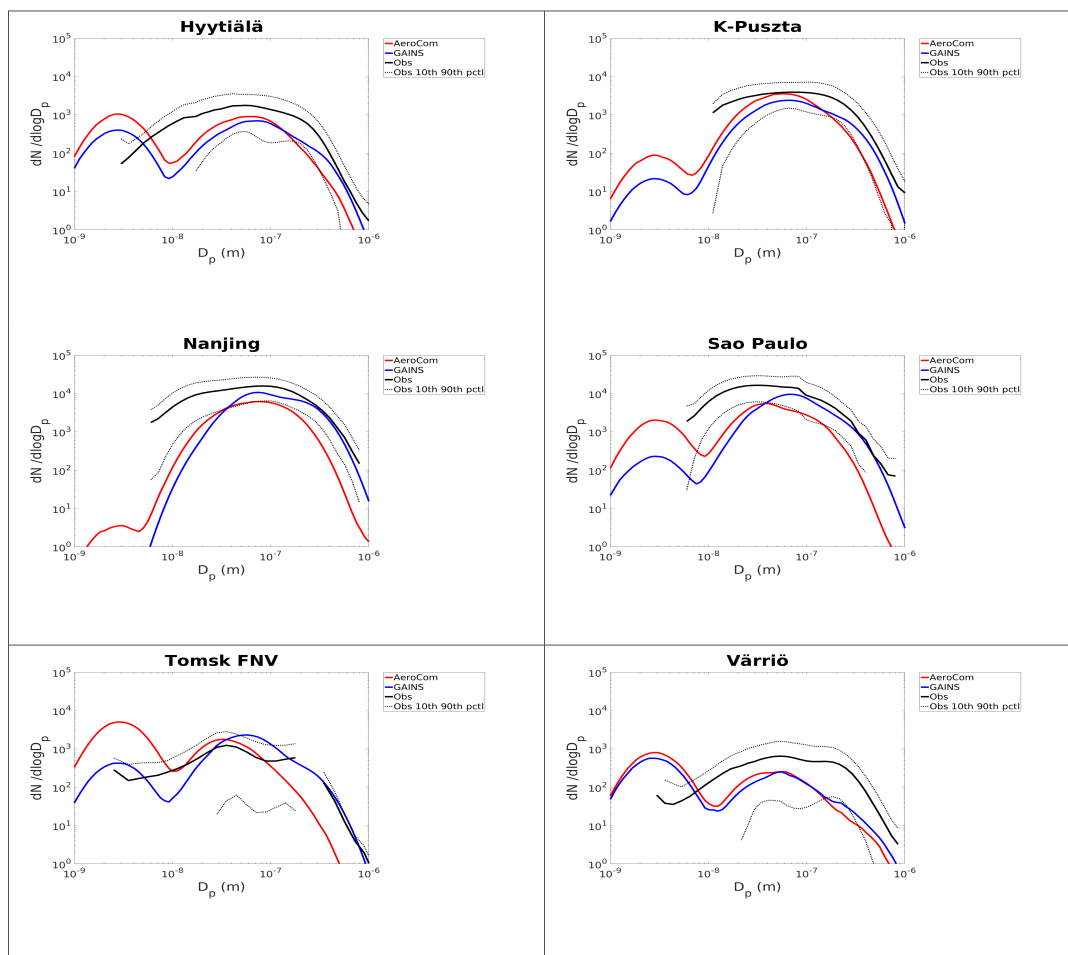
1068



1069 Figure 3. Total absolute emissions for (a) AeroCom and (b) GAINS without visual
1070 interpolation.

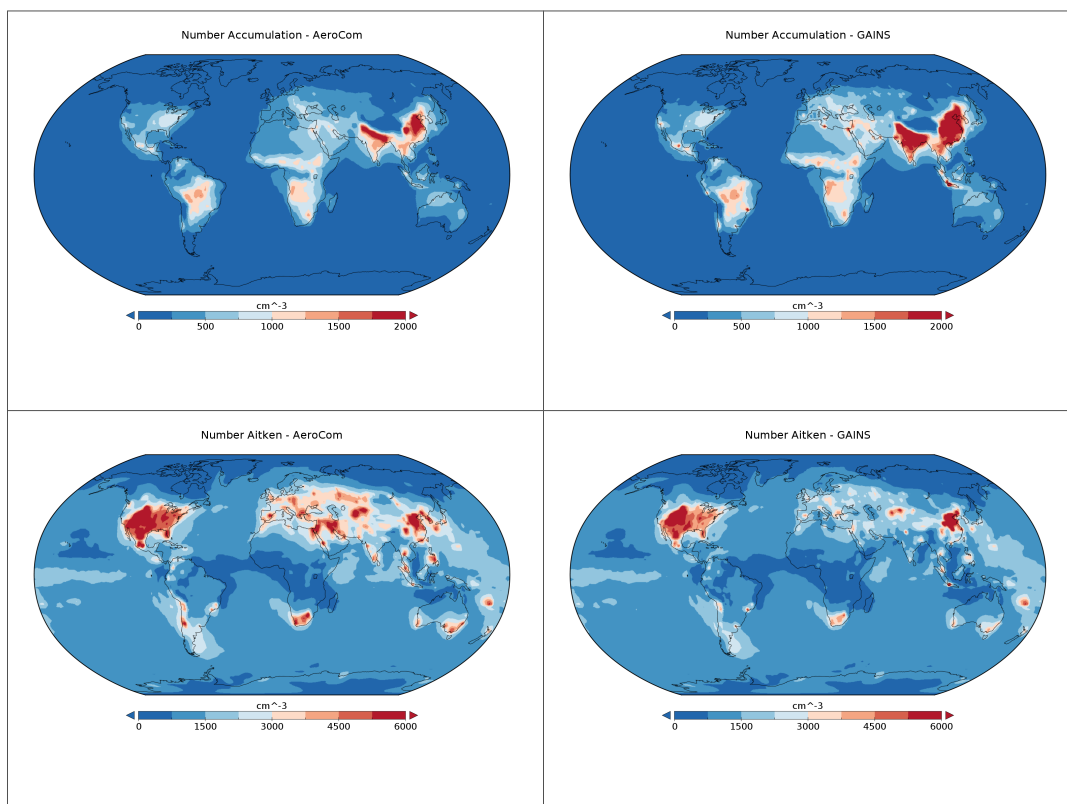


1071 Figure 4. Annual-averaged particle number concentration compared to observational data.
 1072 Measurement sites: 1: Botsalano; 2: Cabauw 3: Hohenpeissenberg; 4: Hyytiälä; 5: K-Pusztá;
 1073 6: Melpitz; 7: Nanjing; 8: Po Valley; 9: Sao Paulo; 10: Tomsk FNV; 11: Värriö. Both plots
 1074 include 1:1 and dashed 1:2, 2:1 lines.



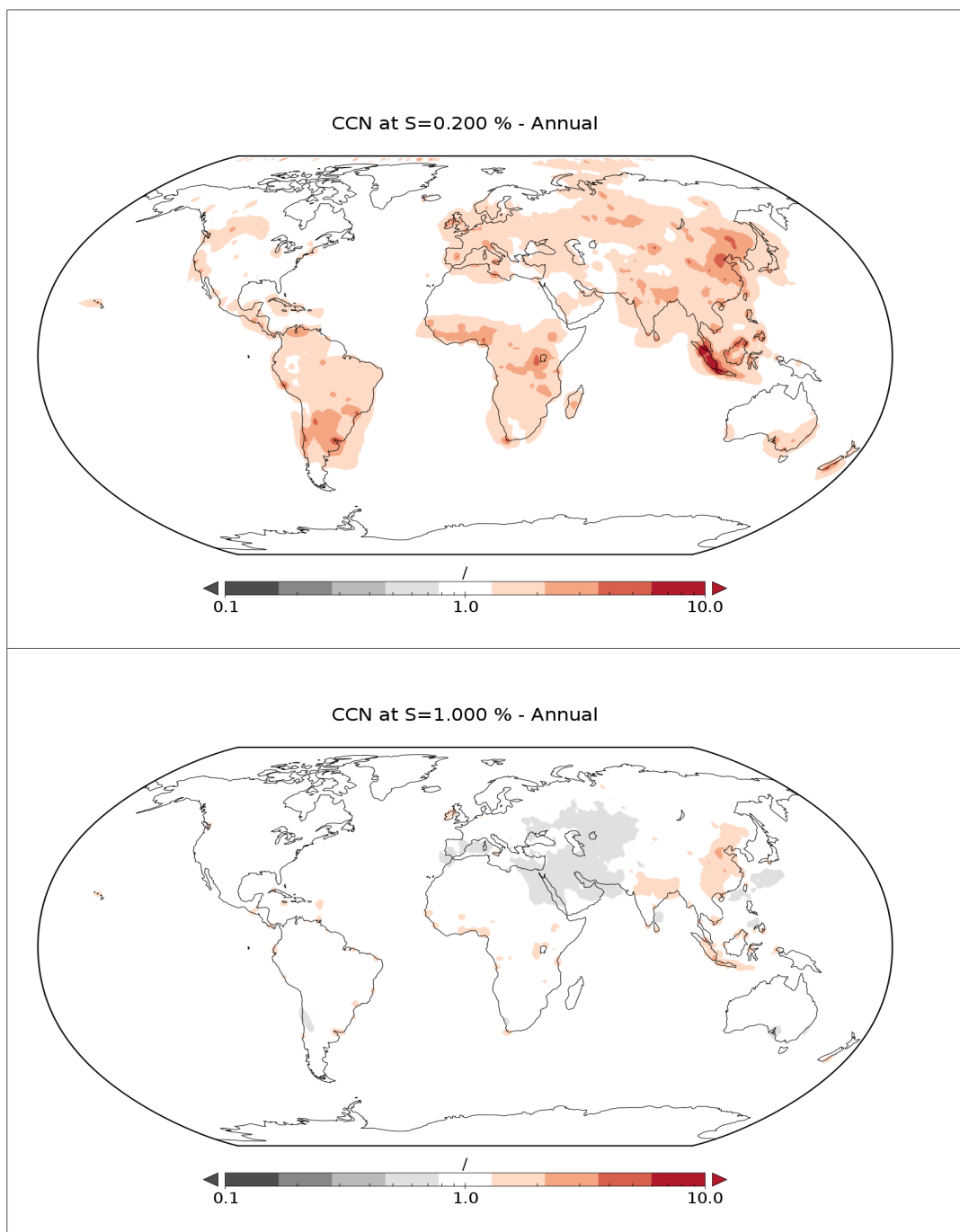
1075 Figure 5. Modeled particle number size distributions compared to observation at 6
1076 measurement sites.

1077
1078
1079

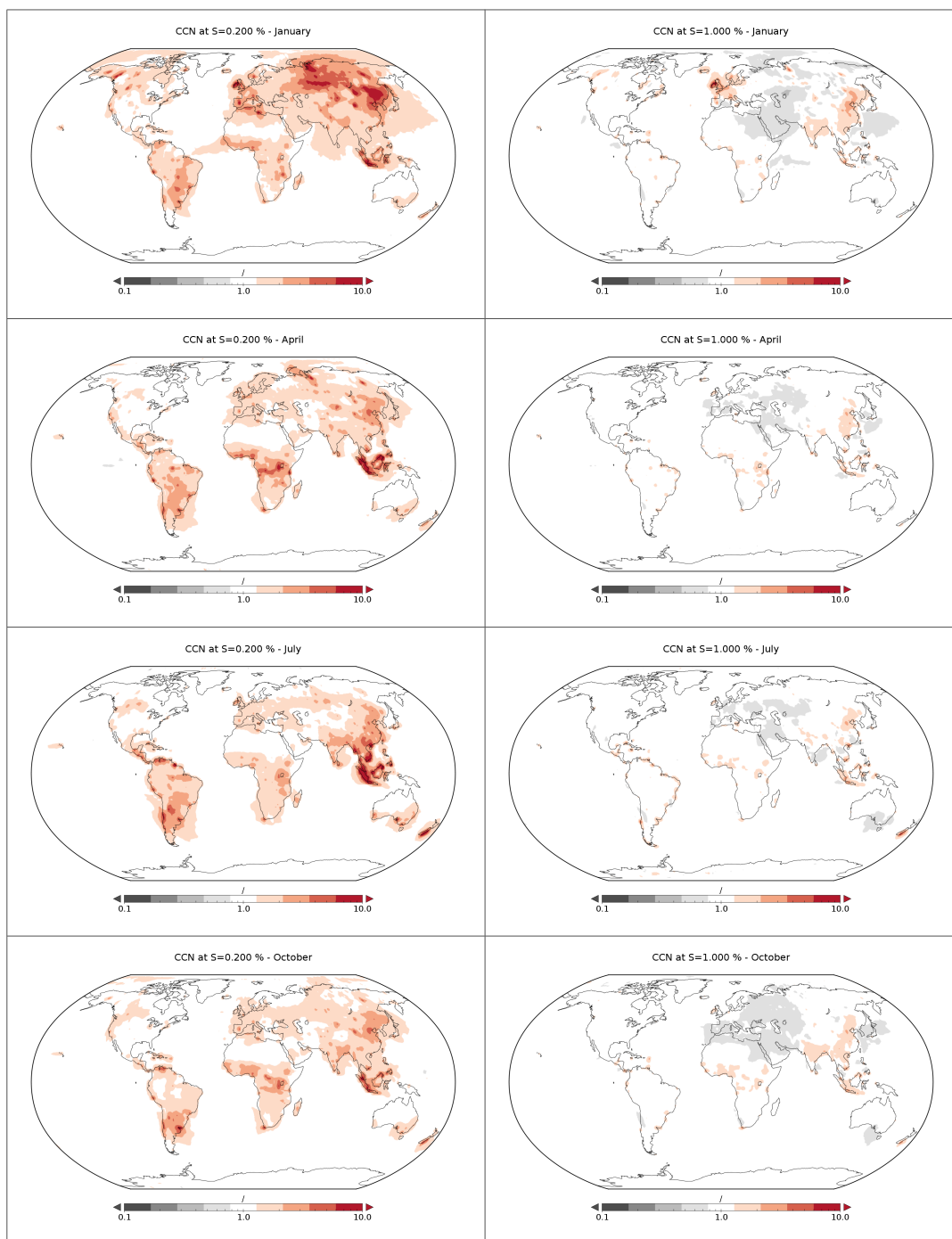


1080 Figure 6. Modeled annual absolute particle number concentrations for accumulation mode
1081 (top) and Aitken mode (bottom).

1082
1083
1084
1085
1086
1087
1088
1089
1090
1091
1092
1093
1094
1095
1096
1097
1098
1099
1100



1101 Figure 7. Modeled annual GAINS/AeroCom ratios of CCN0.2 and CCN1.0.



1102 Figure 8. Modeled seasonal GAINS/AeroCom ratios of CCN0.2 and CCN1.0.